ELSEVIER

Chemical Engineering Journal 72 (1999) 43–51

Chemical Engineering Journal

Three-phase mass transfer with non-linear equilibrium

E. Nagy*

Research Institute of Chemical and Process Engineering, Pannon University of Agricultural Sciences, Egyetem u. 2. P.O. Box 125, 8200 Veszprém, Hungary

Received 4 January 1998; received in revised form 21 September 1998; accepted 6 October 1998

Abstract

A new model has been developed to describe the curve of three-phase mass trasfer with non-linear equilibrium between a continuous and dispersed phases. An improved homogeneous model was applied, which takes into account the diffusion and chemical reaction in the dispersed phase. The non-linear isotherm was correlated by two or three linear segments. The absorption rate can be calculated for all mass-trasfer and reaction kinetic parameters in the case of first- and zero-order reactions. The film-penetration theory was used involving, as limiting cases, the absorption rates for film and surface renewal theories. The model introduced here involves, as limiting cases, previous models known from the literature.

Keywords: Three-phase mass transfer; Pseudo-homogeneous model; Non-linear equilibrium function between the phases

1. Introduction

The absorption of gas into a liquid containing fine solid particles (reactant or catalyst) or droplets is a common process and has been extensively investigated, both theoretically and experimentally [1–12]. In view of the fact that the particles are very small , most pseudo-homogeneous models assume that internal mass transport is instantaneous [2–4,6]. Recently, Nagy and Moser [5] published an improved homogeneous model which includes the effect of internal mass transport and both, first- and zero-order internal and/or external reactions. It was demonstrated that internal mass transport may have a significant effect on the absorption rate even when the particle-size range is very small. The general film-penetration theory was used involving, as limiting cases, both film (surface renewal frequency tends to zero) and surface renewal (film thickness tends to infinity) theories.

The basic assumption of the above-mentioned models is that the solubility (partition) of the compound being absorbed (or adsorbed) shows a linear equilibrium relation between the continuous liquid and the dispersed phases. This, however, may not be generally true. The third, dispersed phase can consist of either organic droplets [10–12] or fine solid particles. In the latter case, when the compound is adsorbed on the solid surface [1,3,7,8,13], non-linearity of the adsorption isotherm should occur in most cases. An example involves the equilibrium relation of dissolved hydrogen between oil and lanthanum–nickel alloy ($LaNi_5$) as fine particles in the oil phase [3,13]. It should be noted that, despite the extensive studies of absorption in three-phase systems, the non-linearity of the equilibrium properties and its effect on the absorption rate have hardly been investigated. Mehra [9] developed a model to predict the absorption rate in a three-phase system with a non-linear isotherm, using the penetration theory. He approximated the non-linear equilibrium curve by piecewise linearization. Using two or three straight lines instead of the non-linear curve, the differential mass balance equations, established for the liquid boundary layer at the gas–liquid interface, are represented by a set of linear equations which can be solved analytically for the cases of zero- or first-order reactions.

The main limitation of Mehra's model is that it does not involve the effects of internal diffusion and chemical reaction on the absorption rate. This is because he assumes that internal mass transport is an instantaneous process. Therefore, the so-called relative-solubility-controlled and external-transport-controlled regimes have to be discussed separately. Thus, his model can only applied in two extreme cases:

1. when external diffusion is rapid (solubility-controlled-regime); and

*Corresponding author. Tel.: +36-88-421-614; fax: +36-88-424-424; e-mail: nagy@mukki.richem.hu

1385-8947/99/$ – see front matter
PII: S1385-8947(98)00140-5

2. when the equilibrium capacity is very high and, consequently, the external diffusion is the so-called rate-determining step (external-transport-controlled regime).

The model does not cover the intermediate range, when both the solubility and external diffusion influence the absorption rate. Moreover, the effects of internal diffusion and internal chemical reaction are also excluded from the model.

By applying the improved homogeneous model [5] for three-phase mass transfer with non-linear equilibrium, a more general model can be derived which contains internal mass transport and, consequently, the two limiting cases mentioned above. This model enables us to calculate the internal concentration distribution of the dispersed phase and its exact effect on the absorption rate. The non-linearity of the solubility curve is again approximated by piecewise linearization. For mass transfer, general film penetration theory was used involving the film and surface renewal theories. The zero- and first-order reactions in both the external and internal phases were taken into consideration.

2. Theory

It is assumed that the particle size of the dispersed phase is small compared with the 'film' thickness, and therefore, a pseudo-homogeneous model can be used for three-phase mass transfer. The equilibrium relation of a compound between solid particles and liquid phase can often be non-linear, because of the non-linear adsorption properties. The shapes of non-linear equilibrium curves can be very different. A typical equilibrium relation is given by the Langmuir isotherm (Fig. 1(A)), but hyperbolic and sigmoidal functions, are also possible. The mathematical treatment methods of these curves do not differ greatly. Each type of curve can be approximated by two or three (or more) linear isotherms as shown in Fig. 1(A) (broken lines). The approximation shown in this figure was obtained by trial and error which, from a practical point of view, seems to be a good approach. The aim of this study is not to present an exact mathematical method from which we can obtain the optimum values of δ_1 (and δ_2). The objective is to obtain the minimal deviation between the original isotherm and the approximation consisting of linear segments.

The slopes of the linear segments (H_i) and the points of intersection (C_i) between them characterize the mathematical equation of the segment lines

$$A_d = H_i(A - A_i) + C_i \tag{1}$$

The differential mass-balance equation for the i_{th} segment of the liquid boundary layer at the gas–liquid interface (e.g. for sections 0 to δ_1, δ_1 to δ_2 and δ_2 to δ in the case of a three-zone model, i=1, 2, 3, respectively) can be given as follows

$$D\frac{\partial^2 A}{\partial x^2} - Q - \frac{J_{d,i}}{a^*}\frac{\omega}{1-\varepsilon} = \frac{\partial A}{\partial t} \quad i = 1, 2 \text{ (and } 3) \tag{2}$$

The initial and boundary conditions for the boundary layer are as follows

$$\begin{aligned} &\text{if } t = 0 \quad \text{and} \quad x > 0 \text{ then } A = 0 \\ &\text{it } t > 0 \quad \text{and} \quad x = 0 \text{ then } A = 1 \\ &\text{if } t > 0 \quad \text{and} \quad x = \delta \text{ then } A^0 = 0 \end{aligned} \tag{3}$$

At the δ_i zone boundaries, which represent the locations of the A_i values (Fig. 1(A)) of the $A(x)$ curve (Fig. 1(B)), the continuity of mass flux exists; consequently, the following conditions are valid at these locations

$$\text{if } t > 0 \text{ and } x = \delta_i, \text{ then } A = A_i \text{ and } \left.\frac{\partial A}{\partial x}\right|_{x=-\delta_i} = \left.\frac{\partial A}{\partial x}\right|_{x=+\delta_i} \tag{4}$$

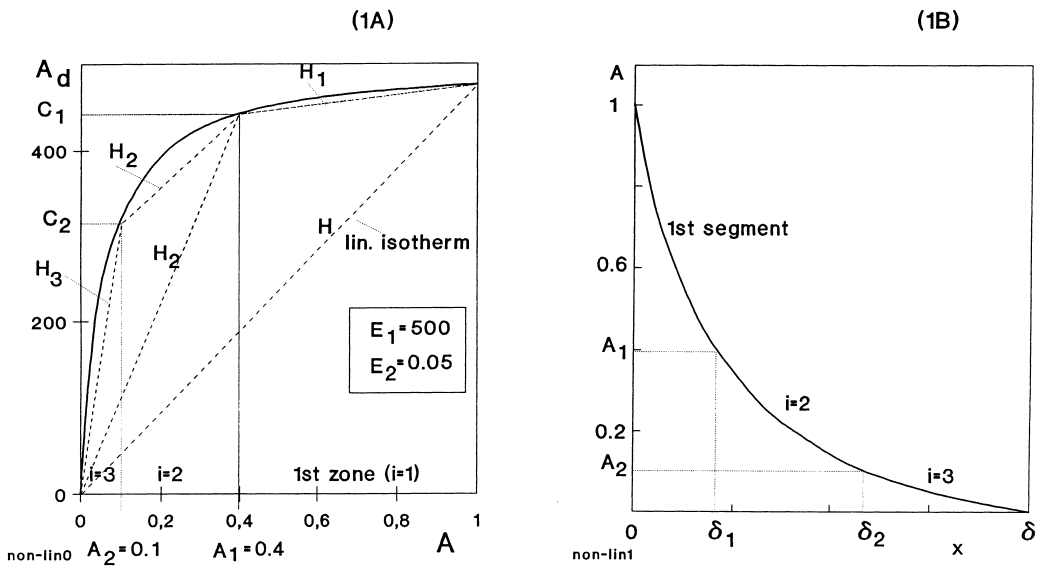

Fig. 1. (A) A non-linear solubility (partition) isotherm (full line) and those approximated by one, two or three linear segments (broken lines). (B) The concentration distribution in the boundary layer $A_d = E_1 A/(E_2 + A)$; E_1=500, E_2=0.05, A_1=0.4, and A_2=0.1.

The case when the bulk concentration is greater than zero, $A_0>0$ has no practical importance for mass-transfer enhancement, and therefore this case is not discussed here (see Nagy [14]).

The key factor in Eq. (2) is the $J_{d,i}$ value which gives the specific mass transfer rate into the particles in the liquid boundary layer at the gas–liquid interface. This was defined by Nagy and Moser [5] for a linear absorption isotherm and for both, zero- and first-order reactions. By applying it to the ith segment, the $J_{d,i}$ value can be given as follows

$$J_{d,i} = B_i A_d a^* \tag{5}$$

For a first-order internal reaction,

$$B_i = \frac{1}{H_i/B^0_{cd} + 1/B_d} \tag{6}$$

$$B_d = \frac{D}{\delta_d}\frac{S}{D_r}\left(\frac{\lambda_d}{\tanh \lambda_d} - 1\right) \tag{7}$$

$$\lambda_d = s^0_d\sqrt{1 + \left(\frac{k_d}{s^0_d}\right)^2} \tag{8}$$

$$B^0_{cd} = \frac{D}{\delta_d}\left(S + \frac{s^0_{cd}}{\tanh s^0_{cd}}\right) \tag{9}$$

with

$$D = \frac{\delta_d}{R};\ k_{1d} = \sqrt{\frac{k_{1d}R^2}{D_d}};\ s^0_d = \sqrt{\frac{sR^2}{D_d}};\ s^0_{cd} = \sqrt{\frac{s\delta_d^2}{D_d}}$$

For a zero-order internal reaction

$$B_i = \frac{1}{H_i/B^0_{cd} + 1/B^0_d(1 + (k_d/s^0_d)^2)} \tag{10}$$

$$B^0_d = \frac{D}{\delta_d}\frac{S}{D_r}\left(\frac{s^0_d}{\tanh s^0_d} - 1\right) \tag{11}$$

with

$$k_d = \sqrt{\frac{k_{0d}R^2}{D_d a^*}}$$

In Eq. (6), B^o_{cd} denotes the external mass-transfer coefficient between the continuous phase and droplets in the gas–liquid boundary layer, while B_d and B^0_d denote the internal mass-transfer coefficients with, and without, chemical reaction, respectively. These coefficients are discussed in detail in an earlier paper by Nagy and Moser [5]. B_i defines the overall mass-transfer coefficient between the continuous and dispersed phase in the gas–liquid boundary layer.

Knowing the values of $J_{d,i}$ and Q ($Q=k_1A$ and $Q=k_0/a^*$ for first- and zero-order reactions in the continuous phase, respectively) in Eq. (2), the set of equations consisting of two or three linear differential equations can be solved analytically by means of Laplace transform. The general solution for the Laplace transform concentration in the ith section can be given as

$$\overline{A} = F_i \exp(\lambda_i X) + F_{i+1}\exp(-\lambda_i X) + \frac{K_i}{s} \tag{12}$$

The values of λ_i, F_i, F_{i+1} and K_i depend not only on the H_i and C_i values, but also on the order of the internal reaction. For a first-order reaction

$$\lambda_i = s^0\sqrt{1 + \frac{M^2}{(\tanh s^0)^2} + \frac{M'^2_i H_i}{(\tanh s^0)^2}} \tag{13}$$

$$K_i = \left(\frac{s^0}{\lambda_i}\right)^2\left(-\frac{M'^2_i}{(\tanh s^0)^2}(C_i - H_i A_i)\right) \tag{14}$$

with

$$M = \frac{\sqrt{k_1 D}}{\beta^0}, \quad M' = \frac{\sqrt{B_i D\omega/(1-\varepsilon)}}{\beta^0}$$

For a zero-order reaction

$$\lambda_i = s^0\sqrt{1 + \frac{M'^2_i H_i}{(\tanh s^0)^2}} \tag{15}$$

$$K_i = \left(\frac{s^0}{\lambda_i}\right)^2\left(-\frac{M^2}{(\tanh s^0)^2} - \frac{M'^2_i}{(\tanh s^0)^2}(C_1 - H_i A_i)\right) \tag{16}$$

with

$$M = \frac{\sqrt{k_0 D/a^*}}{\beta^0}$$

According to the conditions $A=A_i$ and $\partial A/\partial x|_{x=-\delta_i} = \partial A/\partial x|_{x=+\delta_i}$ at δ_i (Eq. (4)), the tangent of the $A(x)$ curve does not change at these points. As a result, these conditions do not lead to a change in the linearity of mass-transport problem. Consequently, the Laplace transformed concentration $\overline{A}$ can be used to determine the average value of the absorption rate. It can be obtained using [15]

$$J = J(t)\exp(-st)\mathrm{d}t \equiv Dsa^*\left.\frac{\mathrm{d}\overline{A}}{\mathrm{d}x}\right|_{x=0} \tag{17}$$

2.1. Two-zone model

According to Fig. 1, the two sections of the boundary layer are the distances from 0 to δ_1 and from δ_1 to δ. This division can be changed arbitrarily. The solution of the set of differential equations consisting of two equations contains five parameters (F_1 to F_4 and δ_1). Using the boundary conditions (Eq. (3)) and the zone boundaries (Eq. (4)), we obtain five algebraic equations which can be solved

by standard mathematical methods. Knowing the F_1 to F_4 and δ_1 values, the absorption rate can be given as

$$J = \frac{D}{\delta_1}\frac{(\lambda_1\delta_1/\delta)}{(\tanh(\lambda_1\delta_1/\delta)}\left[\left(1 - A_1\frac{1}{\cosh(\lambda_1\delta_1/\delta)}\right) - K_1\left(1 - \frac{1}{\cosh(\lambda_1\delta_1/\delta)}\right)\right]a^* \quad (18)$$

The δ_1 value obtained by solution cannot be explicitly expressed; it can be determined from the following implicit equation by trial and error

$$A_1\left(\frac{\lambda_1}{\lambda_2}\frac{1}{\tanh(\lambda_1\delta_1/\delta)} + \frac{1}{\tanh[\lambda_2(1-\delta_1/\delta)]}\right) = \frac{\lambda_1}{\lambda_2}\frac{1}{\sinh(\lambda_1\delta_1/\delta)} - K_1\frac{\lambda_1}{\lambda_2}\left(\frac{1}{\sinh(\lambda_1\delta_1/\delta)} - \frac{1}{\tanh(\lambda_1\delta_1/\delta)}\right) - K_2\left(\frac{1}{\sinh[\lambda_2(1-\delta_1/\delta)]} - \frac{1}{\tanh[\lambda_2(1-\delta_1/\delta)]}\right) \quad (19)$$

2.2. Three-zone model

2.2.1. Film-penetration theory

Here, we have three segments with three differential equations. Altogether there are eight parameters (F_1 to F_6, δ_1 and δ_2) to be determined, and also the same number of boundary conditions at $x=0$, $x=\delta_1$, $x=\delta_2$ and $x=\delta$. The solution obtained, using the film-penetration theory, is rather complicated. Values of δ_1 and δ_2 can be obtained by trial and error via Eqs. (20)–(23) which involve only two independent equations

$$F_4(\delta_1) = -\frac{\exp(\lambda_2\delta_1/\delta)}{2}\left[K_2 - A_1\left(1 - \frac{\lambda_1}{\lambda_2}\frac{1}{\tanh(\lambda_1\delta_1/\delta)}\right) - \frac{\lambda_1}{\lambda_2}\frac{1}{\sinh(\lambda_1\delta_1/\delta)} - K_1\frac{\lambda_1}{\lambda_2}\left(\frac{1}{\tanh(\lambda_1\delta_1/\delta)} - \frac{1}{\sinh(\lambda_1\delta_1/\delta)}\right)\right] \quad (20)$$

$$F_4(\delta_2) = -\frac{\exp(\lambda_2\delta_2/\delta)}{2} \times \left[-K_2 + A_2\left(1 + \frac{\lambda_3}{\lambda_2\tanh[\lambda_3(1-\delta_2/\delta)]}\right) + K_3\frac{\lambda_3}{\lambda_2}\left(\frac{1}{\sinh[\lambda_3(1-\delta_2/\delta)]} - \frac{1}{\tanh[\lambda_3(1-\delta_2/\delta)]}\right)\right] \quad (21)$$

$$F_3(\delta_1) = (A_1 - K_2)\frac{1}{\exp(\lambda_2\delta_1/\delta)} - \frac{F_4(\delta_1)}{(\exp[\lambda_2\delta_1/\delta])^2} \quad (22)$$

$$F_3(\delta_2) = (A_2 - K_2)\frac{1}{\exp(\lambda_2\delta_2/\delta)} - \frac{F_4(\delta_2)}{(\exp[\lambda_2\delta_2/\delta])^2} \quad (23)$$

(For example, at a given value of δ_1, the δ_2 value can be varied in the regime of $\delta_1<\delta_2\leq\delta$ and the values of $F_3(\delta_1)$, $F_3(\delta_2)$, $F_4(\delta_1)$ and $F_4(\delta_2)$ can be calculated using Eqs. (20)–(23). Then, the foregoing calculation can be repeated with a new value of δ_1, until we obtain the correct δ_1 and δ_2 values. This is the case when $F_3(\delta_1)=F_3(\delta_2)$ and $F_4(\delta_1)=F_4(\delta_2)$ are realized). Knowing the δ_1 value, the mass-transfer rate can be given by Eq. (18).

2.2.2. Surface renewal theory

From practical point of view, the three-zone model can be solved using the well-known surface renewal theory. When the film thickness is regarded as infinite ($\delta\rightarrow\infty$), δ_1 and δ_2 can be expressed in separate equations (Eqs. (24) and (25), respectively), and therefore the determination of their values will be much easier. The value of δ_1 can be determined using Eq. (24) and then δ_2 from Eq. (25)

$$\frac{(A_2 - K_2) - T_2}{T_2} = \frac{(A_1 - K_2) - T_1}{T_1} \quad (24)$$

and

$$\delta_2 = \delta_1 + \frac{1}{\lambda_2}\ln\frac{T_1}{T_2} \quad (25)$$

where

$$T_1 = -\frac{1}{2}\left(K_2 - A_1\left[1 - \frac{\lambda_1}{\lambda_2}\frac{1}{\tanh(\lambda_1\delta_1)}\right] - \frac{\lambda_1}{\lambda_2}\frac{1}{\sinh(\lambda_1\delta_1)} - K_1\frac{\lambda_1}{\lambda_2}\left[\frac{1}{\tanh(\lambda_1\delta_1)} - \frac{1}{\sinh(\lambda_1\delta_1)}\right]\right)$$

and

$$T_2 = \frac{1}{2}\left(A_2\left[1 + \frac{\lambda_3}{\lambda_2}\right] - K_2 - K_3\frac{\lambda_3}{\lambda_2}\right)$$

Obviously, the λ_i and K_i values also change in the case of infinite film thickness. The new values can be obtained easily from Eqs. (13)–(16) by substituting $\delta\rightarrow\infty$. For example, for first-order internal and external reactions

$$\lambda_i = \sqrt{\frac{s}{D}(1 + M^2 + M_i'^2 H_i)} \quad (26)$$

$$K_i = -\frac{M_i'^2(C_i - H_i A_i)}{1 + M^2 + M_i'^2 H_i} \quad (27)$$

The mass transfer rate can be given as follows

$$J + \frac{D}{\delta_1}\frac{(\lambda_1\delta_1)}{\tanh(\lambda_1\delta_1)}\left[\left(1 - A_1\frac{1}{\cosh(\lambda_1\delta_1)}\right) - K_1\left(1 - \frac{1}{\cosh(\lambda_1\delta_1)}\right)\right]a^* \quad (28)$$

For completeness, we also give the limiting case (when $\delta\rightarrow\infty$) of Eq. (19) which can be used to calculate the δ_1

value for the two-zone model

$$A_1\left(1+\frac{\lambda_1}{\lambda_2}\frac{1}{\tanh(\lambda_1\delta_1)}\right)=+\frac{\lambda_1}{\lambda_2}\frac{1}{\sinh(\lambda_1\delta_1)} - K_1\frac{\lambda_1}{\lambda_2}\left(\frac{1}{\sinh(\lambda_1\delta_1)}-\frac{1}{\tanh(\lambda_1\delta_1)}\right)+K_2 \quad (19A)$$

3. Results and discussion

A non-linear absorption isotherm and correlation by piecewise linearization (with one, two and three segments) are illustrated in Fig. 1(A). The slopes of the linear segments should be chosen in such a way that the difference between the absorption isotherm and the correlation should be at a minimum. The concentration distribution in the boundary layer is shown in Fig. 1(B).

3.1. The effect of non-linearity on the absorption rate

The model presented enables us to calculate the absorption rate under all mass-transfer and reaction-kinetic conditions. There are several parameters (s, δ, d_p, ϵ, D, k_1, k_0, H) which, in addition to the curvature of the isotherm, influence the absorption rate. The effect of the mass-transfer kinetic parameter $s^0(s^0=\sqrt{s\delta^2/D})$ is particularly important (Fig. 2) Approaches: by one linear isotherm – A_d=476A, $0\leq A\leq 1$; by two linear isotherms – A_d=1125A, $0\leq A\leq 0.4$; A_d=450+43.3(A−0.4), $0.4\leq A\leq 1$; by three linear isotherms: A_d=3250A, $0\leq A\leq 0.1$; A_d=325+417(A−0.1), $0.1\leq A\leq 0.4$; A_d=450+43.3(A−0.4), $0.4\leq A\leq 1$. a change in its value involves film ($s^0<0.3$) and surface renewal ($s^0>3$) theories. The real absorption (or adsorption) isotherm to be linearized (given in Fig. 1(A)) can be defined by the following equation with E_1=500 and E_2=0.05

$$A_d=\frac{E_1A}{E_2+A} \quad (29)$$

(Dividing the numerator and the denominator of this equation by E_2 will give the well-known Langmuir-type adsorption equation.) According to these extreme E_1 and E_2 values, the shape of the isotherm strongly differs from a linear form. Generally, the Langmuir-type isotherm used in this paper can be characterized by two parameters (E_1 and E_2), where E_1 affects, first of all, the 'slope' of the isotherm, while E_2 affects the curvature. As shown in Fig. 1(A), the values of A_1 and A_2 were chosen as 0.4 and 0.1, respectively. The absorption rate was calculated, as shown in Fig. 2, by different approximations of the real isotherm, namely with one, two and three linear segments, as well as without internal reactions (k_d=0) and accompanied by a fast reaction (k_d=5). With increasing value of s^0, the curves reach a maximum for k_d=0. It should be noted that the effect of the third phase on the absorption rate is limited, because D_r=1; thus, it is affected only by the solubility value H, when k_d=0. At smaller values of s^0, the mass-transfer coefficient B_d, and, consequently, the value of J are rather small; at higher values of s^0, the contact time of the liquid elements in the boundary layer will become progressively smaller with increasing s^0 and, accordingly, the mass-transfer rate into the dispersed particle and, as a result, its effect on the absorption rate will be gradually reduced. When k_d>0, increasing values of k_d can provide a higher absorption rate at lower values of s^0. Fig. 2 also illustrates the effect of the goodness of the linearization process on the absorption rate. At the given parameter values, the difference between the absorption rates obtained by approximation with two (curves 2) and three (curves 3) linear segments is not significant. The approximation with one straight line gives very poor results (curves 1). Obviously, the shape of the non-linear isotherm affects the goodness of the piecewise linearization approach and, thus, the value of the calculated absorption rate obtained.

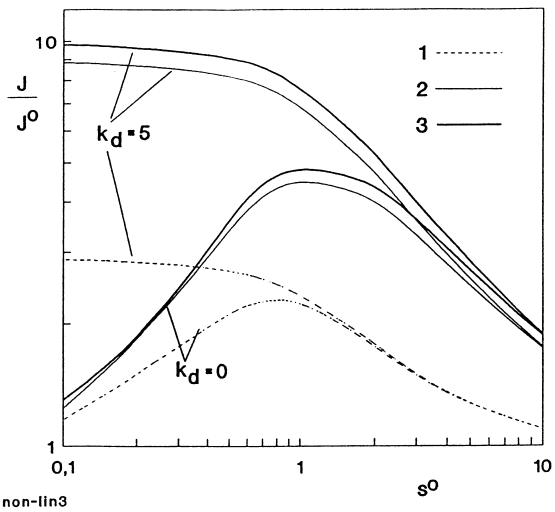

Fig. 2. The influence of the different correlations of the real isotherm given in Fig. 1 (A_d=500A/(0.05+A)) on the absorption rate as a function of s^0 (S=4.5, ϵ=0.1, δ_r=1, D_r=1, and M=0).

The effect of the parameters of the real absorption isotherm, E_1 and E_2, on the absorption rate is shown in Fig. 3(A). The linearization was made using two (curves 1) and three (curves 2) straight lines, and the absorption rate is related to that obtained by approximation with one linear curve J_{lin}, as given in Figs. 1 and 3(B). The latter figure illustrates the change in shape of the isotherm at different values of E_2. As can be seen, at higher values of E_2, when the curvature of the isotherm is decreasing with increasing E_2 value, the value of J/J_{lin} tends to unity. By increasing the curvature of the isotherm on decreasing the value of E_2, the value of J/J_{lin} also increases. Similarly, the difference between the approximations with two and three linear curves will be greater with increasing value of E_1 and decreasing value of E_2. The data shown in Fig. 3(A) may explain the large difference between the measured and predicted absorption rates of gases in aqueous, activated

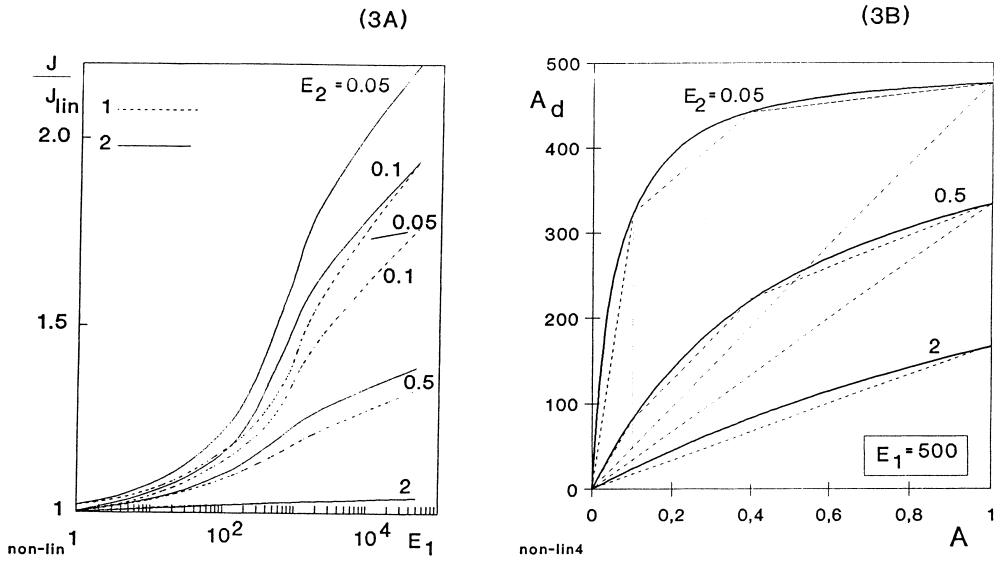

Fig. 3. (A) The effect of parameters E_1 and E_2 on the absorption rate relative to that obtained using one linear isotherm. (B) The shape of the non-linear isotherms at E_1=500. (S=10, ϵ=0.1, δ_r=1, D_r=1, k_d=0, M=0, A_1=0.4, A_2=0.1.). 1, Approximation by two linear isotherms; and 2, approximation by three linear isotherms.

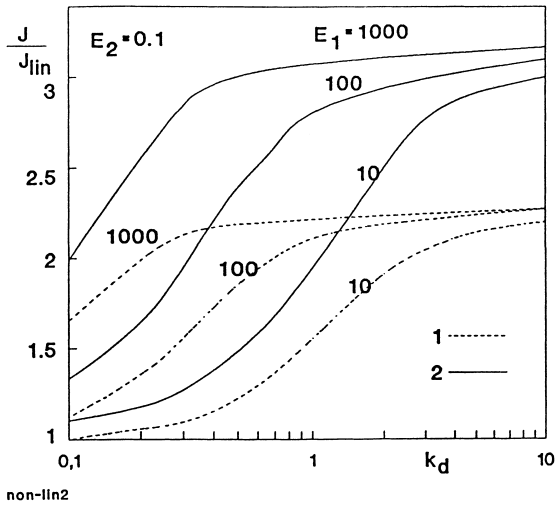

Fig. 4. The effect of internal chemical reaction on the absorption rate (S=10, ϵ=0.1, δ_r=1, D_r=1, M=0, A_1=0.4, A_2=0.1). 1, Approximation by two, and 2, approximation by three linear isotherms.

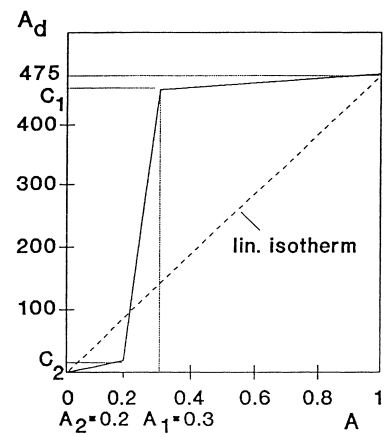

Fig. 5. The correlation of the absorption isotherm of hydrogen on $LaNi_5$ alloy in silicone oil slurry by three linear segments (at 25°C), [3]. The three linear segments can be given by the following equations (C_1=468, C_2=2, A_1=0.3, A_2=0.2): A_d=10A, 0≤A≤0.2, i=3; A_d=[2+4660(A−0.2)], 0.2≤A≤0.3, i=2; A_d=[468+10(A−0.3)], 0.3≤A≤1, i=1.

carbon slurries, published by Holstvoogd et al. [2]. They reported that the measured absorption rates were much higher than the predicted ones. This anomaly might, at least partly, be caused by the non-linearity of the adsorption isotherm.

The effect of non-linearity in the presence of an internal chemical reaction (k_d>0) is also very interesting (Fig. 4). With an increase in the internal chemical reaction rate, the effect of the shape of the isotherm on the absorption rate decreases. As can be seen, the difference between the results obtained by the two different methods is rather high, and also increases with increasing internal reaction rate. At very high values of k_d, the curves tend to a limiting value. In this rate regime, the amount of absorbed compound diffused into the particles reacts completely and, therefore, the external mass transfer coefficient B^0_{cd} will be the so-called rate-determining step.

On the basis of results shown here, it can be concluded that the approximation with two linear isotherms yields, from a practical point of view, an acceptable absorption rate. Therefore, the more complicated three-curve approximation need only be used in special cases.

3.2. An example of the applicability of the model

Holstvoogd et al. [3] reported data on the absorption rate of hydrogen into slurries of $LaNiH_x$ alloy. According to their results, the real absorption isotherm should be very close to

Table 1
Absorption rate of hydrogen (with non-linear isotherm) into $LaNi_5$ suspension in silicone oil (d_p=7 μm, k_d=0, ϵ=0.06, M=0, D_r=1, the maximum value of a_d=3.88×10^4 mol/m^{-3} belonging to a^*=84–73 mol/m^{-3} (25–75°C), H=3.88×10^4/a* – Henry's constant for linear isotherm related to the whole concentration range)

T	β^0	D	s	s^0	S	J/J^0	
(°C)	10^{-4} (m/s)	10^{-9} (m^2/s)	(s^{-1})	—	—	measured	calculated
25	3.7	2.5	0.6	0.1	1.9	1.08	1.11
40	4.24	3.44	0.7	0.12	2.3	1.19	1.18
55	5.26	4.5	1.2	0.15	2.5	1.24	1.27
70	6.18	5.7	5.7	0.3	2.7	1.89	1.96

the approximation with three linear segments as shown in Fig. 5. The exact value of A_1 (and A_2) is not given by the authors, but it should be equal to 0.3. The mathematical expressions of the segments are listed in Fig. 5. The values of the mass-transfer kinetic parameters (β^0, D, J/J^0, a^*, etc.) taken from Ref. [3] are given in Table 1. As shown in Fig. 2, the s^0 value has a strong effect on the absorption rate. For the determination of s^0, the values of the surface renewal frequency (s) and the film thickness (δ) must be known. In the paper by Holstvoogd et al. [3], only the value of the mass-transfer coefficient, β^0, is given. Based on their experimental conditions (low stirring rate to provide a flat gas–liquid interface and a relatively low value of enhancement of the absorption rate in spite of the large amount of H_2 absorbed in the alloy particles) it can be concluded that the value of the surface renewal frequency is low; it should fall in the film theory range, i.e. $s^0 \leq 0.3$. This is also confirmed by the calculated absorption rates. At higher values of s^0, the enhancement of hydrogen absorption obtained by the presented model was essentially higher than that observed experimentally. The calculated absorption rate and the parameter values of s and S ($S=\delta_d/3.5\times10^{-6}$ m, $d_p=7\times10^{-6}$ m) used for this calculation are listed in Table 1. The values of s and δ were chosen for the calculation in such a way that the $\beta_0 = \sqrt{Ds}/\tanh s^0$ value should be equal to the experimental value given in Table 1.

The δ values during the calculation were kept almost constant, δ=8–9 μm, except for the value used at 25°C, namely δ=6.7 μm. The δ has only a limited effect on the absorption rate, but the surface-renewal frequency strongly alters the J value. Therefore, the s value was varied during the calculation of J, using trial and error. The values of the surface-renewal frequency thus obtained are rather low, between 0.6 and 5.7 s^{-1}. Consequently, the average residence time of particles in the gas–liquid boundary layer is in the range 0.18–1.7 s. The characteristic diffusion time for particles t_D can only be estimated as follows: $t_D=R^2/D_{eff}$ with $R=3.5\times10^{-6}$ m and $D_{eff}=D_0/\tau$ (D=(2.5–5.7)×10^{-9} m^2 s) (the exact values of the porosity (θ) and tortuosity (τ) for this alloy are not known; in general, for porous catalytic particles, θ=0.3–0.5 and τ=2–6 [16]). Using intermediate values for θ and τ, the t_D value changes between 0.02 and 0.05 s in the 25–70°C range. This means that there is sufficient time for particles to become saturated with hydrogen in the boundary layer. The maximum value of the hydrogen concentration in the particles is 3.8×10^4 mol m^3 [3], while the amount of $LaNi_5$ reactant in the particles, with $\rho=7\times10^{-3}$ kg m^{-3}, is 3.5×10^4 mol m^{-3}. Thus, the particles located in the boundary layer can react completely after saturation without additional H_2 adsorption. As a result, the internal chemical reaction does not affect the absorption rate. This is why the J values in Table 1 were calculated for the case of k_d=0. (The film and surface-renewal theories, as limiting cases of the film-penetration theory, were also used for verification, but the results obtained were not satisfactory; J/J^0=1.2–1.4 for the film theory and J/J^0=1.4–1.7 for surface renewal theory between 25° and 70°C).

As can be seen, the calculated and experimental absorption rates are in excellent agreement. The results calculated by the model presented here fit the experimental values better than those obtained by Mehra's model, where the calculated J/J^0 values range between 1.17 and 1.23 (column 9 in Table 1 in Mehra's paper [9]), which differ from the experimental data in Table 1. This proves that the model presented here is suitable for the description of three-phase absorption with non-linear absorption or adsorption isotherms. The results presented here do not allow us to draw exact conclusions about the applicability of the model; further experiments are needed using a simpler surface-renewal theory.

4. Conclusions

The pseudo-homogeneous model presented here is a three-phase mass-transfer model which enables the user to calculate the absorption rate, when a non-linear absorption (or adsorption) isotherm of the absorbed component exists between the continuous liquid and dispersed liquid (or solid) phases. The model takes into account not only the external diffusion and chemical reaction, but also the internal values, i.e. inside the particles or drops in the boundary layer. It was demonstrated by the model that the curvature and slope of the non-linear equilibrium curve can strongly affect the absorption rate. For practical purposes, the simpler two-zone model also gives suitable results. From the model equations, it is very easy to obtain the mass-transfer

rates corresponding to film theory and surface-renewal theory, as limiting cases, i.e. $s \to 0$ and $\delta \to \infty$, respectively.

Acknowledgements

This work was financially supported by the Hungarian Research Foundation under Grant No T 15864.

Appendix

Nomenclature

a	concentration of absorbed compound A in the boundary layer (mol m^{-3})
a_d	concentration of A in the particles (mol m^{-3})
a^*	concentration of A at the gas–liquid interface (mol m^{-3})
a_d^*	concentration of A at the particle interface (mol m^{-3})
A	a/a^*
A_d	a_d/a^*
A_i	concentration of A at the intersection points of the linear segments (i=1, 2, and 3)
A^0	concentration of A in the bulk phase
$\overline{A}$	Laplace transform of concentration A ($\overline{A} = \overline{a}/a^*$)(s)
B_i	overall mass-transfer coefficient for first- and zero-order reactions, respectively (Eqs. (6) and (10)) (m s^{-1})
B_{cd}^0	physical mass-transfer coefficient between the continuous and dispersed phases in the gas–liquid boundary layer defined by Eq. (9) (m s^{-1})
B_d	internal mass-transfer coefficient for first-order reaction of particles (Eq. (7)) (m s^{-1})
B_d^0	internal physical mass-transfer coefficient (Eq. (11)) (m s^{-1})
C_i	constant for the ith linear segments
d_p	particle diameter (m)
D, D_d	diffusion coefficient of absorbed component in the continuous and dispersed phases, respectively (m^2 s^{-1})
D_{eff}	effective diffusion coefficient (m^2 s^{-1})
D_r	D/D_d
E_1, E_2	constants of the Langmuir-type absorption isotherm given in Eq. (29)
F_i	parameters in Eq. (12) given by Eqs. (20)–(23)
H	Henry's law solubility (partition) constant between the continuous and dispersed phases for a linear isotherm related to the whole concentration range ($H=a_d/a$)
H_i	Henry's law constant for i_{th} segment
J	absorption rate (mol m^{-2}s^{-1})
J^0	absorption rate without particles, (mol m^{-2} s^{-1})
J_{lin}	absorption rate obtained by assuming a linear equilibrium relation for the whole concentration range (mol m^{-2} s^{-1})
$J_{d,i}$	mass transfer rate between the continuous and dispersed phases in the ith segment (mol m^{-2} s^{-1})
k_1, k_0	reaction rate constants in the continuous phase for first- and zero-order reactions, respectively (s^{-1}, mol m^{-3} s^{-1})
k_{1d}, k_{0d}	reaction rate constants for the dispersed phase (s^{-1}, mol m^{-3} s)
k_d	$\sqrt{k_{1d}R^2/D_d}$ or $\sqrt{k_{0d}R^2/(D_d a^*)}$, dimensionless reaction rate constant for particles
K_i	defined by Eqs. (14)–(16) for zero- and first-order reactions, respectively
M	$\sqrt{k_1 D/\beta^0}$ or $\sqrt{k_0 D/A^*/\beta^0}$, reaction diffusion parameter (Hatta number) for boundary layer
M_i'	$\sqrt{B_i D\omega/1-\varepsilon}/\beta^0$, modified Hatta number
Q	reaction rate (s^{-1})
R	radius of particles (m)
s	surface-renewal frequency (s^{-1})
s^0	$\sqrt{s\delta^2/D}$, dimensionless time for liquid element in the boundary layer
s_d^0	sR^2/D_d, dimensionless time for particles
s_{cd}^0	$\sqrt{s\delta_d^2/D_d} = s^0/\delta_r$, dimensionless time for boundary layer around the particles
S	spherical coefficient, $S=\delta_d/R$
t	time (s)
t_D	characteristic diffusion time for particles (s)
x	space coordinate (m)
X	x/δ, dimensionless space coordinate

Subscript

i	ith segment of the non-linear isotherm

Greek letters

β^0	physical mass-transfer coefficient, $\beta^0=Ds^0/(\delta \tanh s^0)$ (m s^{-1})
δ	thickness of boundary layer at the gas–liquid interface (m)
δ_d	thickness of boundary layer around the dispersed particles (m)
δ_i	thickness of the ith segments in the boundary layer
δ_r	δ/δ_d
ϵ	hold-up of the dispersed phase
λ_i	defined by Eqs. (13)–(15) for first- and zero-order reactions, respectively
θ	porosity of catalyst particles
ρ	density of particles (kg m^{-3})
τ	tortuosity factor
ω	specific surface of the dispersed phase ($\omega=6\epsilon/d_p$) (m^2 m^{-3})

References

[1] E. Alper, W.D. Deckwer, Comments on gas absorption with catalytic reaction, Chem. Engng. Sci. 36 (1981) 1097.

[2] R.D. Holstvoogd, W.P.M. van Swaaij, L.L. van Dierendonck, The absorption of gases in aqueous activated carbon slurries enhanced by adsorbing on catalytic particles, Chem. Engng. Sci. 43 (1988) 2181.

[3] R.D. Holstvoogd, K.J. Platinski, W.P.M. van Swaaij, Penetration model for gas absorption with reaction in a slurry containing fine insoluble particles, Chem. Engng. Sci. 41 (1986) 867.

[4] A. Mehra, Intensification of multiphase reactions through the use of a microphase I. Theoretical, Chem. Engng. Sci. 43 (1988) 899.

[5] E. Nagy, A. Moser, Three-phase mass transfer: improved pseudo-homogeneous model, AIChE J. 41 (1995) 23.

[6] A. Mehra, A. Pandit, M.M. Sharma, Intensification of multiphase reactions through the use of a microphase II. Experimental, Chem. Engng. Sci. 43 (1988) 913.

[7] O.J. Wimmers, R. Paulussen, D.P. Vermeulen, J.M.H. Fortuin, Enhancement of absorption of a gas into a stagnant liquid in which a heterogeneously catalysed chemical reaction occurs, Chem. Engng. Sci. 39 (1984) 1415.

[8] H. Vinke, P.J. Hamersma, J.M.H. Fortuin, Enhancement of the gas-absorption rate in agitated slurry reactors by gas-absorbing particles adhering to gas bubbles, Chem. Engng. Sci. 48 (1993) 2197.

[9] A. Mehra, Gas absorption in slurries of finite-capacity microphases, Chem. Engng. Sci. 45 (1990) 1525.

[10] B. Janakiraman, M.M. Sharma, Solid–liquid and liquid–liquid slow and fast reactions, Chem. Engng. Sci. 40 (1985) 235.

[11] B.H. Junker, T.A. Hatton, D.J.C. Wang, Oxygen transfer enhancement in aqueous/perfluorcarbon fermentation systems I. Experimental observations, Biotechnol. Bioeng. 35 (1990) 578.

[12] J.L. Rols, J.S. Condoret, C. Fonade, G. Goma, Modelling of oxygen transfer in water through emulsified organic liquids, Chem. Engng. Sci. 46 (1991) 1869.

[13] Y. Tung, E.W. Grohse, F.B. Hill, Kinetics of hydrogen absorption in stirred metal hydride slurry, AIChE J. 32 (1986) 1821.

[14] E. Nagy, Three-phase mass transfer, Thesis for doctor of science. Veszprém, 1994 (in Hungarian).

[15] G.F. Froment, K.D. Bischoff, Chemical Reactor Analysis and Design, Wiley, New York, 1979.

[16] C.N. Satterfield, Mass Transfer in Heterogeneous Catalysis, M.I.T. Press, Cambridge, MA, 1970.